Platform to discover protease-activated antibiotics and application to siderophore-antibiotic conjugates

Jonathan H. Boyce,[1,2] Bobo Dang,[3,*] Beatrice Ary,[1] Quinn Edmondson,[1] Charles S. Craik,[1] William F. DeGrado,[1,2,*] and Ian B. Seiple[1,2,*]

[1.] Department of Pharmaceutical Chemistry, University of California, San Francisco, San Francisco, California 94158, United States
[2.] Cardiovascular Research Institute, University of California, San Francisco, San Francisco, California 94158, United States
[3] Structural Biology of Zhejiang Province, School of Life Sciences, Westlake University, 18 Shilongshan Road, Hangzhou 310024, Zhejiang Province, China.

Abstract.

Here we present a platform for discovery of protease-activated prodrugs and apply it to antibiotics that target Gram-negative bacteria. Because cleavable linkers for prodrugs had not been developed for bacterial proteases, we used substrate phage to discover substrates for proteases found in the bacterial periplasm. Rather than focusing on a single protease, we used a periplasmic extract to find sequences with the greatest susceptibility to the endogenous mixture of periplasmic proteases. Using a fluorescence assay, candidate sequences were evaluated to identify substrates that release native amine-containing payloads without an attached peptide "scar". We next designed conjugates consisting of: 1) an N-terminal siderophore to facilitate uptake; 2) a protease-cleavable linker; 3) an amine-containing antibiotic. Using this strategy, we converted daptomycin – which by itself is active only against Gram-positive bacteria – into an antibiotic capable of targeting Gram-negative *Acinetobacter* species. We similarly demonstrated siderophore-facilitated delivery of oxazolidinone and macrolide antibiotics into a number of Gram-negative species. These results illustrate this platform's utility for development of protease-activated prodrugs, including Trojan horse antibiotics.

Introduction.

The well-recognized term, "ESKAPEE" (previously ESKAPE),[1] encompasses the names of seven species of clinically relevant pathogens (*E. faecium*, *S. aureus*, *K. pneumoniae*, *A. baumannii*, *P. aeruginosa*, *Enterobacter sp.*, and *E. coli*) that are associated with resistance to commonly prescribed antibiotics and are largely responsible for the world's nosocomial infections.[2] Five of these pathogens are Gram-negative species, whose outer membrane and associated resistance-nodulation-cell division (RND) efflux pumps render them resistant to many classes of antibiotics.[3] Indeed, the outer membrane shields the bacteria from molecules that are unable to pass through porins,[4] providing an effective barrier to many molecules that would otherwise be effective antibiotics against these pathogens.[5] Gram-negative therapies can be delivered by siderophore-mediated antibiotic delivery using Nature's Trojan-horse approach.[6-8] Siderophores are small-molecule chelators that are produced by bacteria to sequester Fe(III),[9] which is an essential nutrient required for bacterial growth and virulence.[10] In the case of Gram-negative pathogens, outer membrane proteins (*e.g.* TonB-dependent transporters)[11] bind to iron-chelated siderophores and provide opportunities for facilitated transport.[12,13] Owing to the promiscuity of their transport systems, bacteria also use siderophores in warfare against other microbes.[12,14] For example, Streptomycetes produce albomycins (Figure 1), which are natural siderophore-antibiotic conjugates (SACs) and highly effective antibiotics against Gram-negative *Enterobacteriaceae*.[15] Albomycins are recognized by siderophore uptake machinery, transported into the cytoplasm, and activated by peptidase N, which cleaves the N-terminal serine-amide bond (Figure 1) and releases the t-RNA synthetase inhibitor (blue) to bind to its target.[16-19] Here we extend this strategy by developing an unbiased platform for the discovery of linkers that are cleaved by periplasmic proteases,[20] which demonstrates that this platform can produce SACs with both broad and narrow spectra of activity.

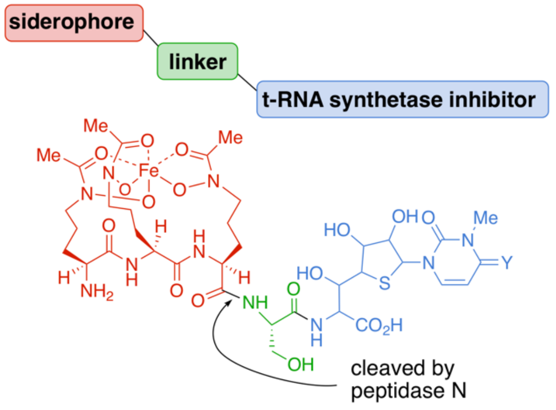

albomycins (Y=O, NH, or NCONH$_2$)

Figure 1. Albomycins, natural siderophore-antibiotic conjugates with peptidase-cleavable linkers.

There are two categories of SACs, depending on the type of linker they possess: non-cleavable and cleavable. There has been significant progress in the development of non-cleavable SACs,[21,22b,23] with the first siderophore–β-lactam conjugate recently approved by the FDA.[24] However, their use is often limited to periplasmic-targeting antibiotics (e.g. daptomycin, vancomycin, and β-lactams). The few examples of cytoplasmic-targeting, non-cleavable SACs may be less effective than the parent antibiotic for two reasons:[25,26b-d,27-34] 1) the conjugate may not pass through the inner membrane to reach the cytoplasm, or 2) the bulky siderophore component may interfere with binding to the target.[12,25b,35] Therefore, cleavable linkers are traditionally thought to be required for SAC compatibility with cytoplasmic-targeting antibiotics.[36] The majority of Gram-positive antibiotics are cytoplasmic-targeting and may require a cleavable linker if they were to be converted into SACs for Gram-negative pathogens.[12,36,37]

Despite extensive work over the last thirty years, only a few cleavable linker strategies have been developed for SACs and a number of challenges remain.[22,25-27,35,36,38-40] Despite optimization for hydrolytic stability,[35] ester linkers for SACs (*e.g.* **A**, Figure 2) are susceptible to premature cleavage prior to bacterial-cell entry.[25,26c-d,27,35,40] SACs with disulfide (*e.g.* **B**) and trimethyl-lock linkers based on reduction- (*e.g.* **C**) and esterase-triggered cleavage mechanisms were less active than the parent antibiotic.[26,39] Recent work by Nolan demonstrated siderophore degradation by the cytoplasmic hydrolase IroD in two uropathogenic strains with a non-cleavable linker.[38] Miller and coworkers developed the β-lactam linker **D** that releases a Gram-positive antibiotic upon ring-opening of the β-lactam ring and subsequent fragmentation.[22a] Importantly, with few exceptions,[22a,27,40] cleavable SACs incorporate a DNA-gyrase-inhibiting fluoroquinolone antibiotic, ciprofloxacin or norfloxacin,[41,42] which are already active against Gram-negative pathogens but become active only upon hydrolytic release of the parent drug. These SACs provide a method to study siderophore-mediated antibiotic delivery, but do not expand the arsenal of Gram-negative antibiotics.[25,26,35,36,38,39] The lack of cleavable linkers for bacterial proteases is a central reason behind the lack of antibiotic diversity associated with SACs.[36]

A protease-cleavable SAC can be classified as a protease-activated prodrug, which upon proteolytic cleavage of an inactivating peptide leads to the release of an active drug.[43,44] Peptide linkers developed for this activation mechanism in cancer therapy are undergoing clinical trials, one approved by the FDA.[45-48] Most proteolytically activated prodrugs are optimized for cleavage by mammalian proteases, including matrix metalloproteinases (MMPs),[49-51] lysosomal proteases[52-55] (*e.g.* cathepsins and legumain),[46,56-58] and serine proteases (*e.g.* kallikreins),[59,60] which are upregulated in disease (*e.g.* cancer, neurodegenerative disorders, inflammation, etc.).[43,45,61,62] Proteolytically activated prodrugs with cleavable linkers are well-established and include antibody-drug conjugates,[63-69] antibody-antibiotic conjugates,[70,71] peptide-drug conjugates,[72] macromolecular prodrugs,[43,73] and protease-activatable photosensitizers,[74,75] with the cathepsin B-sensitive valyl-citrulline (Val-Cit) linker being the most successful and widely known.[66,68] Although most protease-activated prodrugs target cancer, antibody-antibiotic conjugates are undergoing clinical trials for intracellular bacterial infections associated with difficult-to-treat persisters.[70,71] However, current therapies are limited to the treatment of intracellular *S. aureus*, a Gram-positive pathogen, and the linker is optimized for cleavage by mammalian proteases. Linkers have not been developed for bacterial proteases, which may lead to pathogen-specific therapeutics that conserve the microbiota and broad-spectrum antibiotics that target proteases conserved across multiple species.

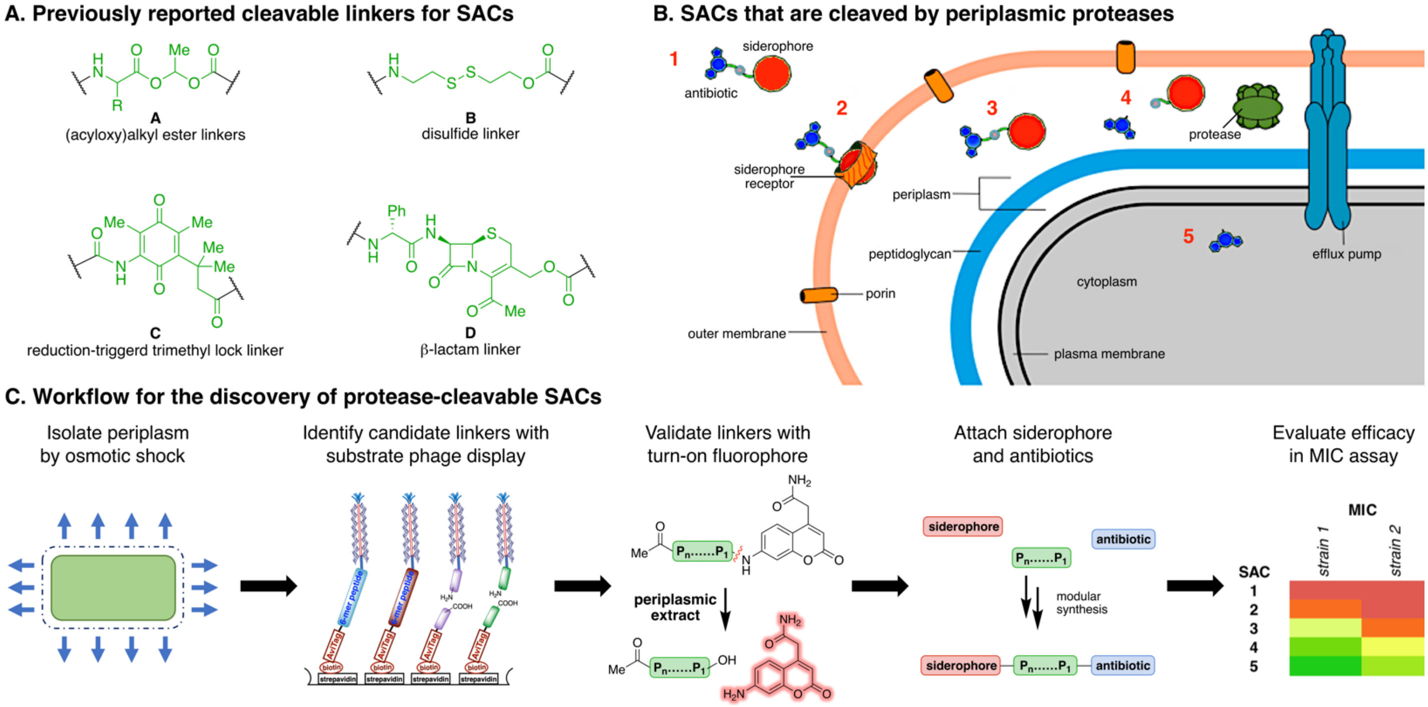

Figure 2. A. Selected cleavable linkers that have previously been used for SACs. **B.** Concept for SACs that contain a linker that can be cleaved by periplasmic proteases. **C**. Workflow for the development of protease-cleavable SACs.

Several technologies have been developed to screen large libraries for protease-substrate profiling,[76] some of which have been successfully applied to prodrug development, such as synthetic combinatorial libraries of fluorogenic substrates,[77,78] positional scanning of synthetic combinatorial libraries,[79,80] substrate phage libraries,[81,82] multiplex substrate profiling by mass spectrometry,[76,83-85] and others.[77,86-90] Given the enormous substrate diversity of fully randomized peptide libraries, substrate phage display[81] provides an unbiased selection tool to discover cleavable linkers for SACs, which can lead to a manageable set of highly specific substrates for a given protease. In contrast to substrate phage display, phage display has been used in vitro and in vivo to design targeted-peptide conjugates.[82] In these efforts, it is common to use mixtures of proteins or whole cells for selection of high-affinity binders.[91] However, substrate phage display has not been applied to prodrug development,[82] and its use for profiling complex biological mixtures is limited.[92] Our work takes full-advantage of substrate phage display to thoroughly explore the substrate specificity of protease mixtures in the bacterial periplasm for the production of protease-cleavable SACs.

In designing protease-activated prodrugs for bacteria-specific proteases, there may be advantages to targeting multiple proteases over an individual protease, **as more than one may be responsible for activation of a conjugate in vivo.**[46,93,94] The importance of this concept was brought to light when the *in-vivo* deletion of cathepsin B resulted in drug release from the combined activity of several proteases with overlapping substrate specificity.[95,96] In fact, it might be advantageous to target multiple proteases rather than one individually to minimize the possibility of resistance when designing antibiotic prodrugs. Thus, we screened broadly for peptides that are cleaved by the multiple proteases present in an unfractionated periplasmic extract. Moreover, the convenience of isolating the periplasmic extract enhances throughput by eliminating the need for expression and purification of specific proteases.

Results.

Substrate Phage Display Leads to WSPKYM–RFG and WSWC–KWASG as Substrates for Periplasmic Cleavage. To discover efficient peptide substrates using the method of substrate phage,[85] we built a random hexapeptide library genetically fused to the pIII gene of M13. A phagemid vector allows monovalent display of the corresponding protein on the tip of the phage. A GGS spacer was incorporated at each end of the randomized peptide to enhance flexibility. An AviTag® sequence was also incorporated at the N-terminus for biotinylation of the displayed peptides. The biotin is used to immobilize the phage library on a streptavidin-coated surface, and a protease can then cleave at favorable peptide sequences. Proteolysis releases the phage, which are then amplified and sequenced to determine the favorable substrates for the protease of interest.

The process of "biopanning" entails the following steps: 1) enzymatic biotinylation of the AviTag® sequence,[97,98] 2) immobilization of the biotinylated library on streptavidin 96-well plates, 3) cleavage of the immobilized library by incubation with the periplasmic extract of *E. coli K12 MG1655* at 37 °C, 4) amplification of the eluted phage using *E. coli TG-1* cells, and 5) isolation and purification of phage for the next round of selection. The periplasmic extract used in panning was obtained by osmotic shock of *E. coli K12 MG1655.*[99] We carried out four rounds of selection (Figure 3), with the stringency being increased with each succeeding round by reducing the amount of extract and decreasing the incubation time. The phagemid from the input library and final round of biopanning were isolated, barcoded, and submitted for Next Generation Sequencing.[100] Sequences for further characterization were ranked based on the extent of enrichment relative to the original library (Table 1).

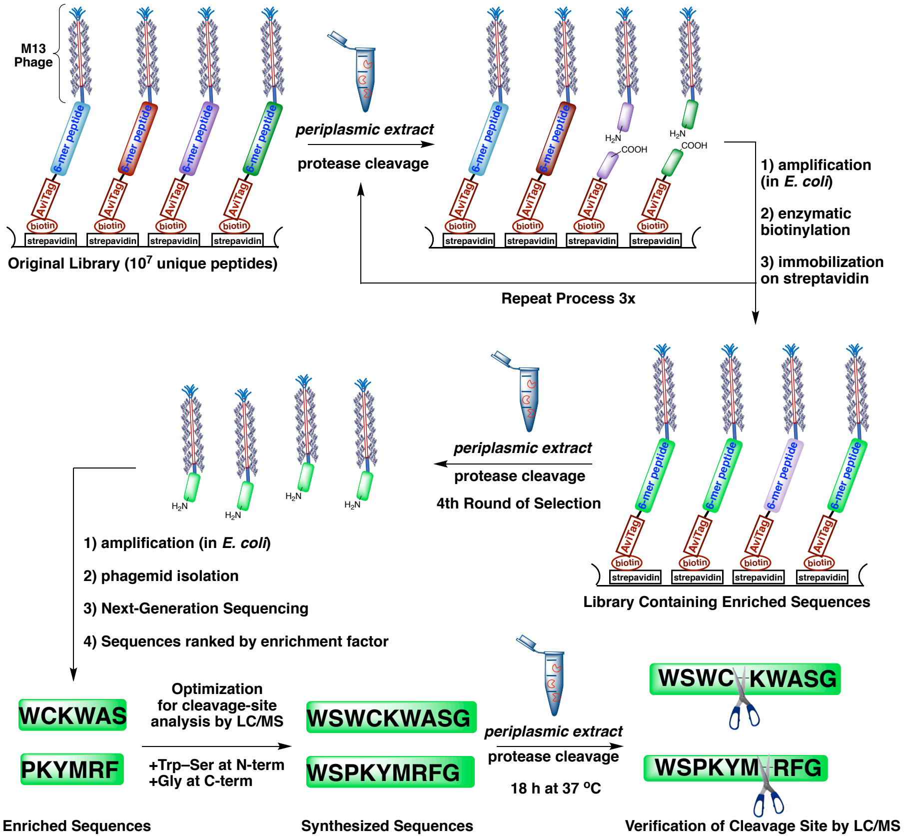

Figure 3. Substrate phage display leads to optimal sequences for cleavage in the periplasmic extract of *E. coli K12 MG1655.*

Sequence	Reads	Initial reads	Enrichment Factor
KNQSLG	10652	0.5	21304
GSDSSV	9239	0.5	18478
NHADVH	8138	0.5	16276
KSEMLS	7742	0.5	15484
WCKWAS	15307	1	15307
PKYMRF	13192	1	13192

Table 1. Highly enriched sequences found through substrate phage display.

Six highly enriched sequences (SKNQSLGG, SGSDSSVG, SNHADVHG, SKSEMLSG, SWCKWASG, and SPKYMRFG) were synthesized with flanking amino acids to mimic the GGS spacers in the phage library. A tryptophan was added to the N-terminus to facilitate detection by HPLC. Each peptide was found to be cleaved to varying extents following treatment with periplasmic extract for 18 h at 37 °C. The cleavage sites and extent of proteolysis were evaluated by LC/MS (Table S5), which revealed that the sequences WSPKYM–RFG (dash – indicates site of cleavage) and WSWC–KWASG may be optimal linkers for cleavable SACs.[100] In addition to their promising cleavage profiles described in Table S5, the presence of these sequences in the original library contributed to their selection as potential linker candidates. In protease substrate nomenclature, the Cys and Met residues at the C-terminal side of the cleavage site are designated as the P1 positions, while the Lys and Arg residues at the N-terminal side are designated as the P1' positions. Although the residues on the P' side are sometimes important for efficient cleavage,[101] this is not always the case.[102]

WSPKYM conjugates are efficiently cleaved without a P' peptide. With the candidate sequences WSPKYM–RFG and WSWC–KWASG in-hand, we asked whether the residues on the C-terminal P' sequence were required for proteolysis. The lack of a P' peptide sequence is considered to be advantageous for prodrugs in which a drug is linked to the P1 residue *via* an amide bond, releasing the parent drug without an appended peptide "scar" that might adversely affect its biological activity (Figure 4A). To probe this question, we used a solid-phase method to synthesize fluorescent substrates in which 7-amino-4-carbamoylmethylcoumarin (ACC) was coupled directly to the P1 Cys or Met residue as an antibiotic surrogate (See Supporting Information).[105,106] We were indeed pleased to find that peptide **1**, which contains the WSPKYM-coumarin sequence was efficiently cleaved by treatment with a periplasmic extract of *E. coli K12* (100 µg/mL total protein) at 37 °C ($t_{1/2}$ = 5.3 ± 0.1 hr). On the other hand, peptide **2** (WSWC-coumarin) was cleaved 25-fold less rapidly under these conditions (Figure 4B). Thus, WSPKYM was determined to be more suitable than WSWC for the development of cleavable SACs.

Design and synthesis of SACs that incorporate daptomycin, an oxazolidinone, and solithromycin. To explore the versatility of SACs, we selected three structurally and mechanistically diverse antibiotics that act on targets in either the periplasm or the cytoplasm. Each antibiotic has an amine, which can be unmasked upon proteolysis of the WSPKYM linker. The lipopeptide daptomycin (**4**) interacts with the cytoplasmic membrane in Gram-positive bacteria, leading to increased membrane permeability and membrane depolarization.[105a-c] However, it is ineffective against Gram-negative bacteria and challenging to functionalize without loss of potency.[105d] Nevertheless, the Miller group has shown that daptomycin can gain activity in Gram-negative species if conjugated to a siderophore with a non-cleavable linker.[22b,23] Here, we examine the use of a protease-cleavable linker.

We also chose two ribosomal protein synthesis inhibitors, amino-oxazolidinone **5** and solithromycin **6**, as examples of antibiotics that must gain access to the cytoplasm to be active.[22a] Since both oxazolidinones and macrolides bind deep within the large ribosomal subunit in fairly occluded binding sites, siderophore conjugates without cleavable linkers have been met with limited success, potentially due to interference of the linkers with binding.[12,21,37,106,107] Our strategy would avoid this complication by enabling release of the parent antibiotics.

For attachment to the N-terminal side of the linker, we sought a siderophore that was synthetically accessible, had a low molecular weight, and was compatible with a variety of bacterial siderophore uptake systems. The bis-catecholate, azotochelin-like[108] siderophore (Miller Siderophore, Scheme 1)[22] was selected due to its ease of synthesis and its ability to carry large cargo (*e.g.* daptomycin) into *A. baumannii*, *E. coli*, and *P. aeruginosa*.[22,23] We used a modified version of Miller's protocol to access siderophore **10**, which has acid-labile ketal protecting groups that can be removed concomitantly with *tert*-butyl and *tert*-butoxycarbonyl (Boc) protecting groups on the amino acid sidechains.[100]

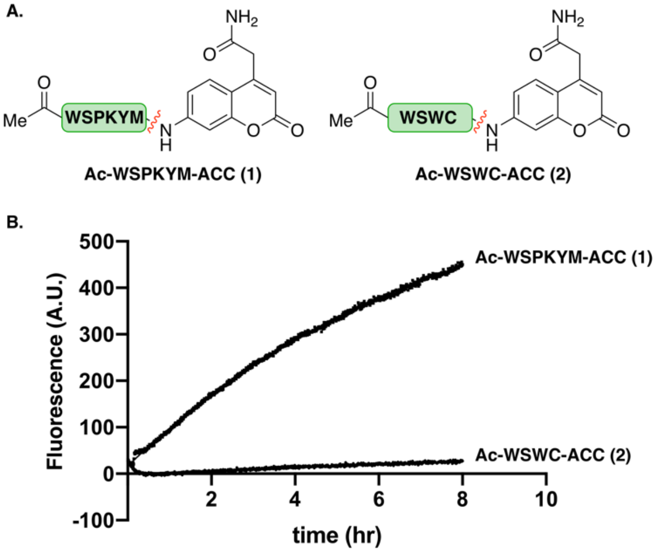

Figure 4. Evaluation of cleavage in periplasmic extract using linker–fluorophore conjugates. Continuous fluorescent assay of the cleavage of antibiotic–fluorophore conjugates by *E. coli* K12 extract. 25 µL of extract (Total Protein: 200 ug/mL) was diluted into assay buffer containing 25 µL of cleavage substrate (25 µM). Cleavage of the amide bond between the peptide and the 7-amino-4-carbamoylmethylcoumarin releases the free coumarin derivative, which is brightly fluorescent. The time course for **Ac-WSPKYM-ACC** (**1**) is well described by a pseudo-first order process with a half-life of 5.3 ± 0.1 hr.

We developed a modular synthetic route that enables the facile incorporation of a variety of linkers, antibiotics, and siderophores (Scheme 1). Gram-scale linker assembly and siderophore attachment were accomplished by solid-phase synthesis to provide the partially protected intermediate **3** in 50% overall yield, and the antibiotic was then coupled to the C-terminus in solution. Following acidolytic deprotection, the final SACs (**7** - **9**) were obtained in 12-53% yield over two to four steps. Several aspects of our route merit further discussion. The majority of the synthesis proceeds on solid phase, simplifying purification and facilitating parallel synthesis of analogues. Antibiotics are directly attached in the penultimate step, enabling rapid access to the final antibiotic conjugates in only two steps from intermediate **3**.[100] The synthesis requires only a single HPLC purification following the coupling step, and the final products are purified by trituration. Daptomycin and solithromycin are commercially available and the oxazolidinones were synthesized following the protocols of Miller[22a] and Rafai Far.[109a]

Scheme 1. Modular synthetic platform for SAC synthesis.

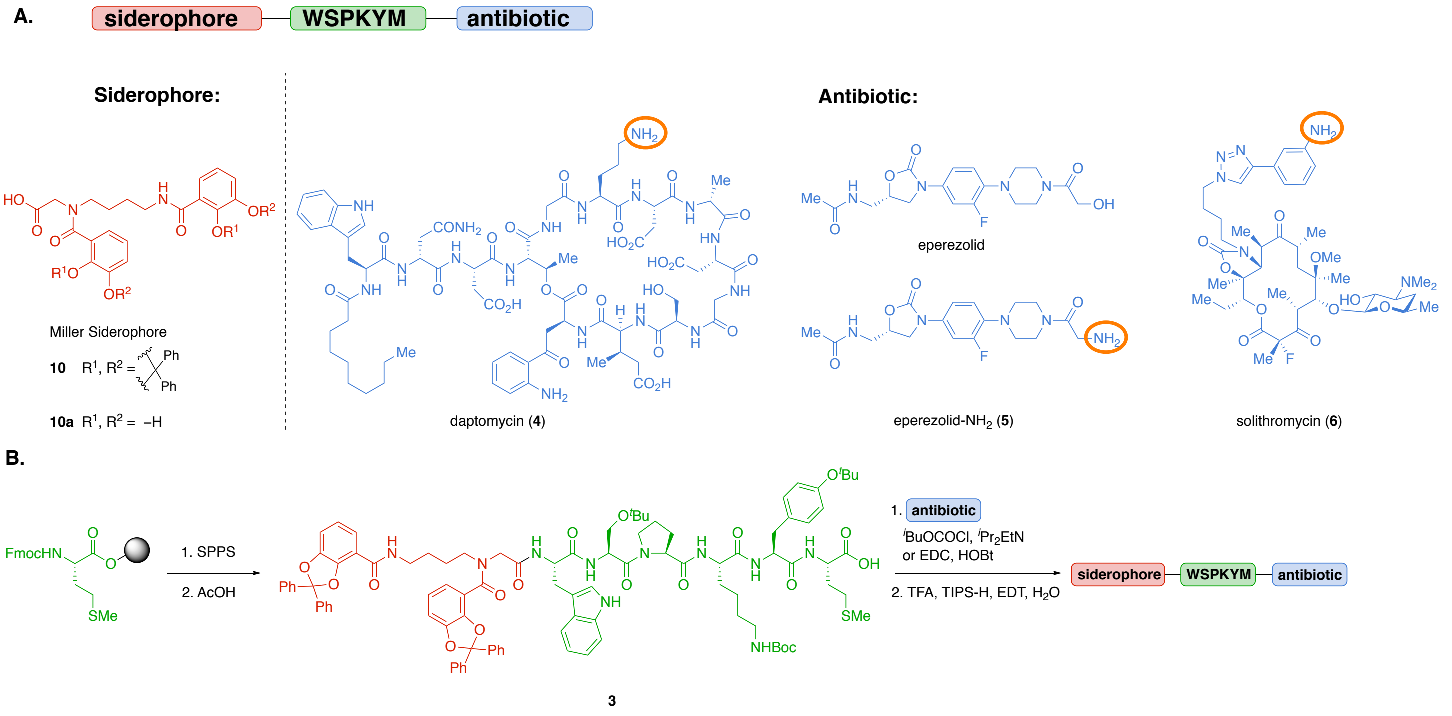

Table 2. Conjugates synthesized in this work.[a]

Compound Number	Designation	N-terminal Substitution	linker	C-terminal Substitution
1	Ac-WSPKYM-ACC	Acetyl	WSPKYM	ACC
2	Ac-WSWC-ACC	Acetyl	WSWC	ACC
7	*L*-Linker Daptomycin Conjugate	Miller Siderophore	WSPKYM	daptomycin (4)
8	*L*-Linker Eperezolid-NH₂ Conjugate	Miller Siderophore	WSPKYM	eperezolid-NH₂ (5)
9	*L*-Linker Solithromycin Conjugate	Miller Siderophore	WSPKYM	solithromycin (6)
11	Conjugate Without Antibiotic, Acid	Miller Siderophore	WSPKYM	free acid (-OH)
12	Conjugate Without Antibiotic, Ester	Miller Siderophore	WSPKYM	methyl ester (-OMe)
13	*D*-Linker Daptomycin Conjugate	Miller Siderophore	wspkym (*D*-linker)	daptomycin (4)
14	*D*-Linker Eperezolid-NH₂ Conjugate	Miller Siderophore	wspkym (*D*-linker)	eperezolid-NH₂ (5)
15	Conjugate With Inactive Enantiomer	Miller Siderophore	WSPKYM	*ent*-eperezolid-NH₂
16	*D*-Linker Solithromycin Conjugate	Miller Siderophore	wspkym (*D*-linker)	solithromycin (6)
17	Conjugate With WSWC Linker	Miller Siderophore	WSWC	eperezolid-NH₂ (5)
18	Conjugate Without Siderophore	Acetyl	WSPKYM	eperezolid-NH₂ (5)

[a] For detailed synthetic methods, see Supporting Information.

We also synthesized several compounds to probe the mechanism of action of **7**, **8**, and **9** using modifications of our existing protocol (**11**-**18**, see Table 2). These included conjugates with *D*-amino acid linkers (*e.g.* **13**, **14**, and **16**)[110] and conjugates that lack an antibiotic or contain an inactive enantiomer of the antibiotic (*e.g.* **11**, **12**, and **15**). To compare the effectiveness of conjugates containing a WSWC linker, which did not cleave effectively in our fluorogenic assay (Figure 4B), we synthesized WSWC conjugate **17**. We also synthesized a siderophore-free conjugate (**18**) to determine the dependence of activity on the siderophore.

Determination of the antibacterial activity of SACs 7-9 and iron-dependent activity. The minimum inhibitory concentrations (MICs) of conjugates **7**-**9** were evaluated according to the standard CLSI antimicrobial susceptibility testing guidelines in Meuller-Hinton-II (MH-II) broth with dipyridyl to sequester iron from the media and promote siderophore-mediated transport (Tables 3-5, S1).[100,111-117] Controls that lacked a siderophore did not show activity-dependence on dipyridyl concentration, while the siderophore conjugate became increasingly active at higher levels of dipyridyl (Table S3A-C). This phenomenon can be explained by the enhanced expression of outer-membrane transport proteins for siderophore uptake in iron-deficient media.[109b] The absence of dipyridyl from the growth medium dramatically attenuated siderophore-conjugate activities without influencing the MIC of the free antibiotic.[100] These results correlate well with expected growth-inhibitory activity of SACs.

We included 15 bacterial strains in our assay (14 Gram-negative and one Gram-positive), and have highlighted selected activities below (for full-activity tables and strain details, see Supporting Information). Two genetically modified strains of *E. coli* were included: a Δ*surA* strain that is deficient in outer-membrane proteins and has increased permeability,[113a] and a Δ*bamB*Δ*tolC* mutant, which has a deficient BamACDE outer-membrane-assembly complex and lacks the TolC-transport protein.[113a,b] This strain is widely used because it is defective in small-molecule efflux.

Antibacterial activity of daptomycin-conjugate 7 (Table 3). Daptomycin is used to treat Gram-positive infections, but it lacks activity against Gram-negative species. Therefore, we were gratified to find that the *L*-linker daptomycin conjugate **7** showed species-specific activity against *Acinetobacter* species and *E. coli,* with MIC values in the 1 to 10 µM range, while daptomycin itself was inactive against these species (MIC > 48 µM). We also measured the activity of **7** against a panel of pathogenic Gram-negative organisms, and found that high activity was observed only for *Acinetobacter* species and *E. coli.* These findings indicate that this approach has the potential to produce Gram-negative antibiotics with relatively narrow-spectrum activity for precision antibiotics. Moreover, as expected, **7** was inactive against *S. aureus,* suggesting that it was not proteolytically activated by this Gram-positive bacterium.

To confirm periplasmic proteolysis of **7** and determine if significant cleavage occurred by a secreted protease, we evaluated the activity of the *D*-linker daptomycin conjugate **13** (in which the chirality of the amino acids in the linker were reversed). Compound **13** was 2 to 10-fold less active than **7** against *E. coli, Acinetobacter baumannii,* and *Acinetobacter nosocomialis.* However, **13** did not entirely lose activity against these species, suggesting that the uncleaved conjugate might have some low level of intrinsic activity against these organisms. Finally, we found that derivatives of **7** lacking the daptomycin payload (**11** and **12**) were essentially inactive, showing only weak activity against the compromised Δ*bamB*Δ*tolC E. coli* mutant. Taken together, these data indicate that we have successfully introduced Gram-negative activity into a derivative of daptomycin, and the enhanced activity of **7** relative to **13** is consistent with our guiding hypothesis of stereospecific proteolytic activation. It is also clear that proteolytic activation likely occurred in the periplasm, rather than by an extracellular protease in the medium, given that daptomycin has no activity against *Acinetobacter baumannii* and *Acinetobacter nosocomialis*.

These results are also of interest with respect to the mechanism of action of daptomycin. It has been previously reported that the target for daptomycin (**4**) may be absent in Gram-negative species due to the differing membrane compositions between Gram-positive and Gram-negative bacteria.[118] Given that **7** is active against *Acinetobacter* and *E. coli*, it would appear that daptomycin is able to act on the cytoplasmic membranes of these Gram-negative species once they gain access. Also, our finding that daptomycin itself is equipotent against *S. aureus Newman* and in the outer membrane-compromised *E. coli ΔsurA* is consistent with this conclusion.

Table 3. Antibacterial activity (MIC in µM) of daptomycin SAC **7** and derivatives thereof.[a]

Daptomycin Conjugates and Controls	***E. coli K12*** wild type	***E. coli* *ΔbamBΔtolC*** efflux knockout	***A. baumannii*** multidrug resistant	***A. nosocomialis*** pathogenic	***E. coli ΔsurA*** outer-membrane knockout	***S. aureus* *Newman*** Gram-positive
Daptomcyin (**4**)	>39	>39	>39	>39	0.6	0.6
L -Linker Daptomycin Conjugate (**7**)	11	11	5	1	>21	>21
D -Linker Daptomycin Conjugate (**13**)	>23	23	23	11	23	>23
Conjugate Without Antibiotic, Acid (**11**)	>48	48	>24	>48	>48	>48
Conjugate Without Antibiotic, Ester (**12**)	>48	24	>24	ND	48	>48

[a] For strain descriptions, see Supporting Information.

Activity of oxazolidinone conjugate 8 in *E. coli* (Table 4). The oxazolidinone class of antibiotics are active against Gram-positive bacteria, but members of this class lack activity against Gram-negative bacteria, due to the presence of endogenous efflux pumps. Nevertheless, mutants of *E. coli* such as *ΔbamBΔtolC* are susceptible to oxazolidinones because these bacterial strains have disruptions in their efflux systems. This strain is susceptible to eperezolid (Table S1), but the corresponding amine variant, eperezolid-NH_2 (**5**) (Table 4), has only minimal activity against *S. aureus Newman.* The low activity of **5** is likely a result of its inability to diffuse through the cytoplasmic membrane rather than intrinsic inactivity against its ribosomal target. We therefore asked whether conjugate **8** could deliver **5** to a *ΔbamBΔtolC* strain of *E. coli.* We were pleased to discover an MIC of 1 µM of **8** for this mutant; the corresponding derivative with an all-*D* linker showed strongly decreased activity with an MIC of 20 µM. Additionally, conjugate **8** displayed no activity in a cell-free translation assay at 38 µM (Figure 5), indicating that the intact conjugate is not capable of directly inhibiting the ribosome. These findings suggest that potent inhibition of bacterial growth requires enzymatic cleavage of the linker. Supporting this suggestion, 34% cleavage of **8** to the parent antibiotic eperezolid-NH_2 occurred after 11–hours of incubation with bacterial periplasmic extract (Table S2). Finally, as expected, conjugate **8** was not active in wild-type strains with functional endogenous efflux pumps (Table S1).

The cleavage of **8** by periplasmic extracts might seem inconsistent with the finding that the corresponding eperezolid-NH_2 (**5**) has only minimal activity (40 μM) against both *E. coli ΔsurA* and *S. aureus*. This finding indicates that the cytoplasmic membrane of both Gram-positive and Gram-negative bacteria provide a barrier for the diffusion of **5** into the cytoplasm. There are two possible explanations for the potent activity of **8** given the lack of activity of **5**: Facilitated transport leads to large differences in the concentrations of molecules in the periplasm versus the cytoplasm, so siderophore-mediated transport into the periplasm could lead to accumulation of **8** and the corresponding cleavage product **5**, enhancing its effective concentration and hence potency. The alternate possibility is that **8** is actively transported to the cytoplasm where it is activated by a cytoplasmic protease.[119]

We also synthesized a number of additional control molecules to probe the antibacterial mechanism of **8**, including conjugate **17** with the WSWC linker, which was found to be inefficiently cleaved in the fluorescent assay. Not surprisingly, this analogue had only weak (MIC = 37 μM) activity, as did compounds **11**, **12**, and **15** that lacked an active antibiotic payload. Similarly, the conjugate **18** without a siderophore was inactive. However, as was the case for some of the daptomycin analogues, a number of the compounds lacking the antibiotic payload retained a modicum of activity (10 - 20 μM), so long as the C-terminus was not negatively charged. This activity was greatest for the derivative with the inactive antibiotic **15** (MIC = 9 μM). We suggest that this activity might occur by a mechanism similar to many non-helical proline-containing cationic antimicrobial peptides.[120] The linker WSPKYM has two aromatic residues known to interact favorably with membranes, a hydrophobic Met and a cationic Lys residue. Also, as is the case for most cationic antimicrobial peptides the introduction of a C-terminal carboxylate decreases antimicrobial activity. Thus, it might be interesting to use the siderophore strategy to deliver short antimicrobial peptides to the cytoplasmic membrane, although such studies are beyond the scope of this work.

Table 4. Antibacterial activity (MIC in μM) and in vitro evaluation of eperezolid-NH_2 conjugate **8** and derivatives thereof.[a]

Eperezolid Conjugates and Controls	***E. coli ΔbamBΔtolC*** efflux knockout	***E. coli ΔsurA*** outer-membrane knockout	***S. aureus Newman*** Gram-positive
Eperezolid-NH_2 (**5**)	>171	43	43
L -Linker Eperezolid-NH_2 Conjugate (**8**)	1	38	>38
D -Linker Eperezolid-NH_2 Conjugate (**14**)	19	>38	>38
Conjugate Without Antibiotic, Acid (**11**)	48	>48	>48
Conjugate Without Antibiotic, Ester (**12**)	24	48	>48
Conjugate With Inactive Enantiomer (**15**)	9	38	>38
Conjugate With WSWC Linker (**17**)	37	ND	ND
Conjugate Without Siderophore (**18**)	>77	ND	>77
% Eperezolid Release From **8** In Extract	34 ± 1.5	ND	ND

[a]For strain descriptions and extract cleavage procedure, see Supporting Information.

Table 5. Antimicrobial activity (MIC in μM) of solithromycin conjugate **9** and derivatives thereof.[a]

Solithromycin Conjugates and Controls	***A. nosocomialis*** pathogenic	***S. typhi*** pathogenic	***S. enterica*** pathogenic	***E. aerogenes*** pathogenic	***K. pneumoniae*** multidrug resistant	***E. coli ΔsurA*** outer-membrane knockout	***S. aureus Newman*** Gram-positive	***E. coli K12*** wild type	***E. coli DCO*** wild type	***E. coli ΔbamBΔtolC*** efflux knockout
Solithromycin (**6**)	5	1	1	9	9	1	1	5	2	1
L -Linker Solithromycin Conjugate (**9**)	7	7	7	7	13	>27	>27	3	7	0.4
D -Linker Solithromycin Conjugate (**16**)	>27	>27	>27	>27	>27	27	>27	3	13	0.8
Conjugate Without Antibiotic, Acid (**11**)	>48	>48	ND	>48	ND	>48	>48	>48	>48	48
Conjugate Without Antibiotic, ester (**12**)	ND	>48	ND	ND	ND	48	>48	>48	ND	24

[a]For strain descriptions and extract cleavage procedure, see Supporting Information.

Solithromycin conjugate 9 has comparable activity to solithromycin in three ESKAPEE pathogens (*E. coli*, *E. aerogenes*, and *K. pneumoniae*) and in *A. nosocomialis* (Table 5). One frequently used strategy to evaluate cleavable SACs involves the use of antibiotic payloads that are already active against Gram-negative pathogens but rendered inactive due to the overall bulk of the SAC.[25,26,35,36,38,39] The successful release of the parent drug can then be conveniently monitored by the emergence of antibacterial activity. We adopted this strategy to examine the release of solithromycin from the *L*-linker SAC **9** and its *D*-linker analogue **16**. The *D*-linker analogue was entirely inactive (MIC > 20 μM) against *A. nosocomialis*, *S. typhi*, *S. enterica*, *E. aerogenes*, and *K. pneumoniae.* In contrast to **16,** the *L*-linker analogue **9** showed robust activity, which is consistent with proteolytic activation in these pathogenic strains.

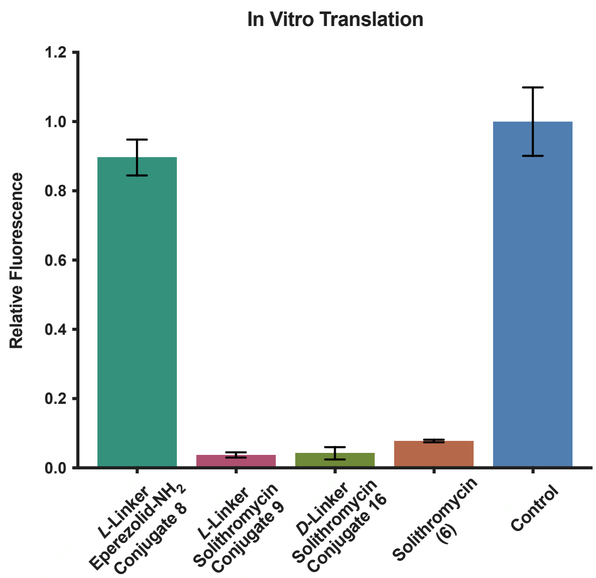

Figure 5. In vitro translation shows the ability of conjugates **8** (38 µM), **9** (10 µM), and **16** (10 µM) to inhibit the 70S *E. coli* ribosome.

When compared to the parent drug, the potencies of **9** ranged from slightly greater than solithromycin to 6-fold less potent, indicating broad specificity to the activation mechanism. Exclusion of DP from the growth medium resulted in loss of activity for solithromycin conjugate **9**, which shows that the activation is not the result of proteolytic cleavage associated with an enzyme in the extracellular medium. If **9** were cleaved in the medium, this would result in the release of solithromycin (**6**), which is active in these strains (Table S3B).

We unexpectedly observed activity of the *D*-linker variant **16** against *E. coli*, which surprisingly had similar activity to its *L*-linker analogue **9**. These results could be explained by the active transport of **16** into the cytoplasm and direct ribosomal inhibition by the conjugate. To investigate this possibility, we conducted an in vitro translation assay with *E. coli* ribosomes (Figure 5), which showed that solithromycin conjugates **9** and **16** inhibit translation in *E. coli* comparable to the free antibiotic at a concentration of 10 µM. These data indicate that cleavage of these conjugates should not be required for activity in *E. coli.*

The lack of *D*-linker activity in Gram-negative species other than *E. coli* is currently under investigation, but might simply reflect differences in the transport systems among Gram-negative species. Conjugates **9** and **16** may not be transported to the cytoplasm in the pathogenic strains,[12,13] thereby requiring linker cleavage for activity. It is anticipated that siderophore transport would be required for solithromycin-conjugate uptake into the cytoplasm due to the inability of **9** and **16** to passively diffuse through the *E. coli* inner membrane since they are not active against the compromised *E. coli ΔsurA*. Structural differences between ribosomes of various species may also contribute to activity variations. Taken together, our results provide strong support for the proteolysis of **9** in five pathogenic strains but also show that a cleavable solithromycin conjugate is not required for activity in *E. coli*.

Conclusions.

The strategy developed here should be broadly applicable for discovery of protease-activated peptide prodrugs for a variety of applications. Here, we focused on delivering antibiotics by designing protease-cleavable siderophore conjugates. By targeting bacterial periplasmic proteases broadly, we were able to design conjugates that act against a broad (or narrow) spectrum of Gram-negative bacteria, illustrating the potential of this approach. Our results provide strong support for the overall mechanism of proteolytic release of the antibiotic from conjugates **7** – **9**. Although we have not yet identified the proteases responsible for activity against our substrates, we purposefully avoided targeting a single protease to decrease the chances of resistance arising from mutants of a single protein. Moreover, the use of chemically stable amide linkers provides an advantage to targeting proteases over esterases and β-lactamases by avoiding the need for esters and β-lactams, which are chemically more labile. Importantly, the modular design and facile synthetic route provides opportunity for rapid variation and evaluation of the siderophore, linker, and antibiotic. This has led to the discovery of cleavable conjugates with activity against several clinically relevant Gram-negative pathogens.

Throughout the course of this work, we made a number of unexpected discoveries with impacts that extend beyond the scope of protease-cleavable prodrugs. Our daptomycin conjugate **7** completely lacks the Gram-positive activity of daptomycin and has gained Gram-negative activity, effectively "flipping" the spectrum of activity of this potent antibiotic. We found that conjugates with *D*-linkers, which are unlikely to be cleaved proteolytically, have moderate activity against several strains of Gram-negative bacteria. Perhaps the most unexpected results are the activities of the solithromycin conjugates **9** and **16** in a cell-free translation assay, which indicate that these large (MW > 2000) conjugates may directly inhibit the ribosome in *E. coli*. These results are extremely surprising in the context of solithromycin–ribosome structural data,[121] and may provide the basis for new macrolide-peptide-hybrid antibiotics.

In summary, this work provides a robust methodology for selection and screening of Trojan-horse prodrugs applied to the persistent and growing problem of antibacterial resistance. Using phage display, one can rapidly screen vast peptide libraries, and by varying the selection strategy one can screen for linkers with desired characteristics. For example, by using periplasmic extracts from different species of bacteria in succeeding selections, one can assure broad activity over the desired range of bacteria. Alternatively, negative selection could be incorporated to select against cleavage of serum proteases or beneficial members of the microbiome. Thus, the potential for fine-tuning the protocol for future practical applications is substantial.

Acknowledgements.

We thank Adam Cotton, Peter Rowheder, Dr. Sam Ivry, and Dr. Matthew Ravalin for helpful discussions. We thank Bruk Mensa for helpful discussions and for providing *P. aeruginosa ATCC 10145*, *S. typhi*, *S. aureus Newman*, *E. coli K12 MG1655*, *E. coli BW25113*

ΔtolC, *E. coli BW25113 ΔsurA*. We thank Neha Prasad for helpful discussions and for providing *K. pneumoniae MGH 78578*, *E. cloacae ATCC13047*, *E. aerogenes ATCC 13048*, *P. aeruginosa PA01*, and *P. aeruginosa PA14*, and *S. enterica 14028s*. We thank Jenna Pellegrino for providing *E. coli BW25113 ΔbamBΔtolC* and for helpful discussions on in vitro translation assays. We thank Professor Joanne Engel for a generous gift of *A. nosocomialis M2*. J.H.B. was supported by the Natural Institutes of Health under the Ruth L. Kirschstein National Research Service Award 5T32HL007731-27 from the National Heart Lung and Blood Institute (NHLBI). Q.E. was supported by the National Science Foundation Graduate Research Fellowship Program under Grant no. 1650113. B.A. was supported by the National Institutes of Health under Grant no. T32 Al 0605357. This project was supported by the David and Lucile Packard Foundation (I.B.S.) and the National Institutes of Health under Grant no. R35 GM122603 (W.F.D.).

Author Information.

Corresponding Authors

ian.seiple@ucsf.edu
bill.degrado@ucsf.edu
dang.bobo@westlake.edu.cn

References

(1) Llaca-Díaz, J. M.; Mendoza-Olazarán, S.; Camacho-Ortiz, A.; Flores, S.; Garza-González, E. One-year surveillance of ESKAPE pathogens in an intensive care unit of Monterrey, Mexico. *Chemotherapy* **2012**, *58*, 475–481.

(2) Pendleton, J. N.; Gorman, S. P.; Gilmore, B. F. Clinical relevance of the ESKAPE pathogens. *Expert Rev. Anti. Infect Ther.* **2013**, *11*, 297–308.

(3) (a) Breijyeh, Z.; Jubeh, B.; Karaman, R. Resistance of Gram-Negative Bacteria to Current Antibacterial Agents and Approaches to Resolve It. *Molecules* **2020**, *25*, 1340–1363. (b) Li, X. Z.; Plésiat, P.; Nikaido, H. The challenge of efflux-mediated antibiotic resistance in Gram-negative bacteria. *Clin Microbiol Rev*. **2015**, *28*, 337–418.

(4) (a) Galdiero, S.; Falanga, A.; Cantisani, M.; Tarallo, R.; Della Pepa, M.E.; D'Oriano, V.; Galdiero, M. Microbe-host interactions: structure and role of Gram-negative bacterial porins. *Curr. Protein Pept. Sci.* **2012**, *13*, 843–854. (b) Nikaido, H. Molecular basis of bacterial outer membrane permeability revisited. *Microbiol. Mol. Biol. Rev.* **2003**, *67*, 593–656.

(5) (a) Choi, U.; Lee, C. R. Distinct Roles of Outer Membrane Porins in Antibiotic Resistance and Membrane Integrity in *Escherichia coli*. *Front. Microbiol.* **2019**, *10*, 953. (b) Braun, V.; Braun, M. Active transport of iron and siderophore antibiotics. *Curr Opin Microbiol.* **2002**, *5*, 194–201. (c) Livermore, D. M. Antibiotic uptake and transport by bacteria. *Scand J Infect Dis Suppl.* **1990**, *74*, 15–22.

(6) (a) Perlman, D. The roles of the Journal of Antibiotics in determining the future of antibiotic research. *Jpn. J. Antibiot.* **1977**, *30*, S201–S206. (b) Diarra, M. S.; Lavoie, M. C.; Jacques, M.; Darwish, I.; Dolence, E. K.; Dolence, J. A.; Ghosh, A.; Ghosh, M.; Miller, M. J.; Malouin, F. Species selectivity of new siderophore-drug conjugates that use specific iron uptake for entry into bacteria. *Antimicrob. Agents Chemother.* **1996**, *40*, 2610–2617. (c) Ji, C.; Juárez-Hernández, R. E.; Miller, M. J. Exploiting bacterial iron acquisition: siderophore conjugates. *Future Med. Chem.* **2012**, *4*, 297–313. (d) Page, M. G. Siderophore conjugates. *Ann. N.Y. Acad. Sci.* **2013**, *1277*, 115–126. (e) Tillotson, G. S. Trojan Horse Antibiotics-A Novel Way to Circumvent Gram-Negative Bacterial Resistance? *Infect. Dis. (Auckl.)* **2016**, *9*, 45–52.

(7) Zheng, T.; Nolan, E. M. Enterobactin-mediated delivery of β-lactam antibiotics enhances antibacterial activity against pathogenic *Escherichia coli*. *J. Am. Chem. Soc.* **2014**, *136*, 9677–9691.

(8) (a) Watanabe, N. A.; Nagasu, T.; Katsu, K.; Kitoh K. E-0702, a new cephalosporin, is incorporated into *Escherichia coli* cells via the tonB-dependent iron transport system. *Antimicrob. Agents Chemother.* **1987**, *31*, 497–504. (b) Curtis, N. A.; Eisenstadt, R. L.; East, S. J.; Cornford, R. J.; Walker, L. A.; White, A. J. Iron-regulated outer membrane proteins of *Escherichia coli* K-12 and mechanism of action of catechol-substituted cephalosporins. *Antimicrob. Agents Chemother.* **1988**, *32*, 1879–1886. (c) Silley, P.; Griffiths, J. W.; Monsey, D.; Harris, A. M. Mode of action of GR69153, a novel catechol-substituted cephalosporin, and its interaction with the tonB-dependent iron transport system. *Antimicrob. Agents Chemother.* **1990**, *34*, 1806–1808. (d) Hashizume, T.; Sanada, M.; Nakagawa, S.; Tanaka, N. Comparison of transport pathways of catechol-substituted cephalosporins, BO-1236 and BO-1341, through the outer membrane of *Escherichia coli.J. Antibiot. (Tokyo)* **1990**, *43*, 1617–1620. (e) Nikaido, H.; Rosenberg, E. Y. . Cir and Fiu proteins in the outer membrane of *Escherichia coli* catalyze transport of monomeric catechols: study with beta-lactam antibiotics containing catechol and analogous groups. *J. Bacteriol.* **1990**, *172*, 1361–1367. (f) McKee, J. A.; Sharma, S. K.; Miller, M. J. Iron transport mediated drug delivery systems: synthesis and antibacterial activity of spermidine- and lysine-based siderophore-beta-lactam conjugates. *Bioconjugate Chem.* **1991**, *2*, 281–291. (g) Dolence, E. K.; Minnick, A. A.; Lin, C. E; Miller, M. J.; Payne, S. M. Synthesis and siderophore and antibacterial activity of N5-acetyl-N5-hydroxy-L-ornithine-derived siderophore-beta-lactam conjugates: iron-transport-mediated drug delivery. *J. Med. Chem.* **1991**, *34*, 968–978. (h) Ji, C.; Miller, P. A.; Miller, M. J. Iron transport-mediated drug delivery: practical syntheses and in vitro antibacterial studies of tris-catecholate siderophore-aminopenicillin conjugates reveals selectively potent antipseudomonal activity. *J. Am. Chem. Soc.* **2012**, *134*, 9898–9901. (i) Kohira, N.; West, J.; Ito, A.; Ito-Horiyama, T.; Nakamura, R.; Sato, T.; Rittenhouse, S.; Tsuji,

M.; Yamano, Y. *In Vitro* Antimicrobial Activity of a Siderophore Cephalosporin, S-649266, against *Enterobacteriaceae* Clinical Isolates, Including Carbapenem-Resistant Strains. *Antimicrob. Agents Chemother.* **2016**, *60*, 729–734.

(9) (a) Miethke, M.; Marahiel, M. A. Siderophore-based iron acquisition and pathogen control. *Microbiol. Mol. Biol. Rev.* **2007**, *71*, 413-451. (b) Hider, R. C.; Kong, X. Chemistry and biology of siderophores. *Nat. Prod. Rep.* **2010**, *27*, 637–657. (c) Chu, B. C.; Garcia-Herrero. A.; Johanson, T. H.; Krewulak, K. D.; Lau, C. K.; Peacock, R. S.; Slavinskaya, Z.; Vogel, H. J. Siderophore uptake in bacteria and the battle for iron with the host; a bird's eye view. *Biometals* **2010**, *23*, 601–611.

(10) (a) Ribeiro M., Simões M. (2019) Siderophores: A Novel Approach to Fight Antimicrobial Resistance. In: Arora D., Sharma C., Jaglan S., Lichtfouse E. (eds) Pharmaceuticals from Microbes. Environmental Chemistry for a Sustainable World, vol 28. Springer, Cham. (b) Ma, L.; Terwilliger, A.; Maresso, A. W. Iron and zinc exploitation during bacterial pathogenesis. *Metallomics,* **2015**, *7*, 1541–1554. (c) Messenger, A. J. M.; Barclay, R. Bacteria, Iron and Pathogenicity. *Biochem. Educ.* **1983**, *11*, 54–63.

(11) Noinaj, N.; Guillier, M.; Barnard, T. J.; Buchanan, S. K. TonB-dependent transporters: regulation, structure, and function. *Annu. Rev. Microbiol.* **2010**, *64*, 43–60.

(12) Wencewicz T. A.; Miller, M. J. Sideromycins as Pathogen-Targeted Antibiotics. *Topics Med. Chem.*; Springer: Berlin, Heidelberg, 2017.

(13) For references discussing the transport of siderophores or siderophore-antibiotic conjugates across the outer and inner membrane of Gram-negative bacteria, see: (a) Page, M. G. P. The Role of Iron and Siderophores in Infection, and the Development of Siderophore Antibiotics. *Clin. Infect. Dis.* **2019**, *69*, S529–S537. (b) Schalk, I. J. Siderophore–antibiotic conjugates: exploiting iron uptake to deliver drugs into bacteria. *Clin. Microbiol. Infect.* **2018**, 24, 801–802. (c) Schalk, I. J.; Guillon, L. Fate of ferrisiderophores after import across bacterial outer membranes: different iron release strategies are observed in the cytoplasm or periplasm depending on the siderophore pathways. *Amino Acids* **2013**, *44*, 1267–1277. (d) Schalk, I.J.; Mislin, G. L.; Brillet, K. Structure, function and binding selectivity and stereoselectivity of siderophore-iron outer membrane transporters. *Curr Top Membr* **2012**, *69*, 37**–**66. (e) Faraldo-Gómez, J. D.; Sansom, M. S. P. Acquisition of siderophores in gram-negative bacteria. *Nat. Rev. Mol. Cell Biol.*, **2003**, *4*, 105–116. (f) Tonziello, G.; Caraffa, E.; Pinchera, B.; Granata, G.; Petrosillo, N. Present and future of siderophore–based therapeutic and diagnostic approaches in infectious diseases. *Infect. Dis. Rep.* **2019**, *11*, 8208.

(14) (a) Wilson, B. R.; Bogdan, A. R.; Miyazawa, M.; Hashimoto, K.; Tsuji, Y. Siderophores in Iron Metabolism: From Mechanism to Therapy Potential. *Trends Mol. Med.* **2016**, *22*, 1077–1090. (b) Holden, V. I.; Bachmann, M. A. Diverging roles of bacterial siderophores during infection. *Metallomics* **2015**, *7*, 986–995. (c) Braun, V.; Pramanik, A.; Gwinner, T.; Köberle, M.; Bohn, E. Sideromycins: tools and antibiotics. *Biometals* **2009**, *22*, 3–13.

(15) Pramanik, A.; Stroeher, U. H.; Krejci, J.; Standish, A. J.; Bohn, E.; Paton, J. C.; Autenrieth, I. B.; Braun, B. Albomycin is an effective antibiotic, as exemplified with Yersinia enterocolitica and Streptococcud pneumoniae. *Int. J. Med. Microbiol.*, **2007**, *297*, 459–469.

(16) Stefanska, A. L.; Fulston, M.; Houge-Frydrych, C. S. V.; Jones, J. J.; Warr, S. R. A potent seryl tRNA synthetase inhibitor SB-217452 isolated from a *Streptomyces* species. *J. Antibiot.* **2000**, *53*, 1346–1353.

(17) For select reports discussing the clinical use of albomycin, see: (a) Gause, G. F. Recent studies on albomycin, a new antibiotic. *Br. J. Med.* **1955**, *2*, 1177–1179. (b) Kaliuzhnaia-Lukashova, G. M. Clinical study of albomycin, colimycin and terramycin. *Klinicheskaia meditsina* **1958**, *36*, 30–5. (c) Georgievskaia, V. S. Clinical observations on the use of albomycin in purulent mastitis. *Sovetskaia meditsina* **1958**, *22*, 82–5. (d) Danovoi, I. D. Use of albomycin in an obstetrical–gynecological clinic. *Akusherstvo i ginekologiia* **1957**, *33*, 37–40. (e) Uglova, V. M. Comparative evaluation of the use of albomycin and furacillin in the treatment of infected wounds; experimental study. *Vestnik khirurgii imeni I. I. Grekova* **1956**, *77*, 73–80. (f) Sigal, A. E. Application of albomycin in the treatment of pulmonary suppurations. *Klinicheskaia meditsina* **1955**, *33*, 24–8. (g) Berent, I. E.; Gil'man, K. Z. Experience in application of the new domestic antibiotic albomycin in dermatovenerology. *Sovetskaia meditsina* **1954**, *18*, 34–5. (h) Raikher, E. A.; El'man, E. F. Application of albomycin in pneumonia in infants during their first months of life. *Sovetskaia meditsina* **1952**, *16*, 18–21. (i) Gamburg, R. L. Use of albomycin in pneumonia in children. *Pediatriia* **1951**, *5*, 37–44. (j) Anonymous author. Antibiotic albomycin in the treatment of pneumonias and toxemias in infants during the first year of life. *Fel'dsher i akusherka* **1951**, *12*, 38. (k) Krechmer B. B.; Val'ter, E. M.; Baiandina, S. A. Application of albomycin in pneumonia in infants. *Sovetskaia meditsina* **1951**, *10*, 10–3.

(18) (a) Zeng, Y.; Kulkarni, A.; Yang, Z.; Patil, P. B.; Zhou, W.; Chi, X.; Van Lanen, S.; Chen, S. Albomycin δ2 Provides a Template for Assembling Siderophore and Aminoacyl-tRNA Synthetase Inhibitor Conjugates. *ACS Chem. Biol.* **2012**, *7*, 1565**–**1575. (b) Fiedler, H.-P.; Walz, F.; Döhle, A.; Zähner, H. Albomycin: Studies on fermentation, isolation and quantitative determination. *Appl Microbiol Biot* **1985**, *21*, 341–347.

(19) Lin, Z.; Xu, X.; Zhao, S.; Yang, X.; Guo, J.; Zhang, Q.; Jing, C.; Chen, S.; He, Y. Total synthesis and antimicrobial evaluation of natural albomycins against clinical pathogens. *Nat. Commun.* **2018**, *9*, 3445.

(20) Merdanovic, M.; Clausen, T.; Kaiser, M.; Huber, R.; Ehrmann, M. Protein quality control in the bacterial periplasm. *Annu. Rev. Microbiol.* **2011**, *65*, 149–168.

(21) For a recent, comprehensive overview of cleavable and non-cleavable SACs, see: Negash, K. H.; Norris, J. K. S.; Hodgkinson, J. T. Siderophore – Antibiotic conjugate design: New drugs for bad bugs? *Molecules* **2019**, *24*, 3314–3330.

(22) For a list of references using the azotochelin-like, Miller Siderophore for SAC development, see: (a) Liu, R.; Miller, P. A.; Vakulenko, S. B.; Stewart, N. K.; Boggess, W. C.; Miller, M. J. A synthetic dual drug sideromycin induces gram-negative bacteria to commit suicide with a gram-positive antibiotic. *J. Med. Chem.* **2018**, *61*, 3845–3854. (b) Ghosh, M.; Lin, Y-M.; Miller, P. A.; Mollmann, U.; Boggess, W.

C.; Miller, M. Siderophore conjugates of daptomycin are potent inhibitors of carbapenem resistant strains of *Acinetobacter baumannii*. *J. ACS Infect. Dis.* **2018***, 4,* 1529–1535. (c) Miller, M. J.; Lin, Y.-M.; Ghosh, M.; Patricia, A.; Moellmann, U. Antibacterial Sideromycins. Int. Patent Application PCT/IB2015/056915, February 25, 2016. (d) Miller, M. J.; Cheng, I. J. Antibacterial Monobactams. Int. Patent Application PCT/US2018/053917, April 11, 2019. (e) Carosso, S.; Liu, R.; Miller, P. A.; Hecker, S. J.; Glinka, T.; Miller, M. J. Methodology for Monobactam Diversification: Syntheses and Studies of 4-Thiomethyl Substituted -Lactams with Activity Against Gram–Negative Bacteria, Including Carbapenemase Producing *Acinetobacter baumannii*. *J. Med. Chem.* **2017**, *60*, 8933-8944.

(23) Ghosh, M.; Miller, P. A.; Möllman, U.; Claypool, W. D.; Schroeder, V. A.; Wolter, W. R.; Suckow, M.; Yu, H.; Li, S.; Huang, W.; Zajicek, J.; Miller, M. J. Targeted antibiotic delivery: selective siderophore conjugation with daptomycin confers potent activity against multidrug resistant *Acinetobacter baumannii* both *in vitro* and *in vivo*. *J. Med. Chem.* **2017**, *60*, 4577–4583.

(24)https://www.fda.gov/news-events/press-announcements/fda-approves-new-antibacterial-drug-treat-complicated-urinary-tract-infections-part-ongoing-efforts

(25) For examples of (acyloxy)methyl ester linkers with low hydrolytic stability, see: (a) Hennard, C.; Truong, Q. C.; Desnottes, J.-F.; Paris, J.-M.; Moreau, N. J.; Abdallah, M. A. Synthesis and Activities of Pyoverdin-Quinolone Adducts: A Prospective Approach to a Specific Therapy Against Pseudomonas aeruginosa. *J. Med. Chem.* **2001**, *44*, 2139–2151. (b) Rivault, F.; Liébert, C.; Burger, A.; Hoegy, F.; Abdallah, M. A.; Schalk, I. J.; Mislin, G. L. A. Synthesis of pyochelin–norfloxacin conjugates. *Bioorg. Med. Chem. Lett.* **2007**, *17*, 640–644. (c) Noël, S.; Gasser, V.; Pesset, B.; Hoegy, F.; Rognan, D.; Schalk, I. J.; Mislin, G. L. A. Synthesis and biological properties of conjugates between fluoroquinolones and a N3′′-functionalized pyochelin. *Org. Biomol. Chem.* **2011**, *9*, 8288–8300.

(26) For examples of esterase-, phosphatase-, and reduction-triggered linkers for fluoroquinolone release, see: (a) Miller, M. J.; Cheng, I. J. Reduction-Triggered Antibacterial Sideromycins. U.S. Patent application US 2016/0368878 A1, April 23, 2016. (b) Ji, C.; Miller, M. J. Siderophore-fluoroquinolone conjugates containing potential reduction-triggered linkers for drug release: synthesis and antibacterial activity *Biometals,* **2015**, *28*, 541–551. (c) Fardeau, S.; Dassonville-Klimpt, A.; Audic, N.; Sasaki, A.; Pillon, M.; Baudrin, E.; Mullié, C.; Sonnet, P. Synthesis and antibacterial activity of catecholate–ciprofloxacin conjugates. *Bioorg. Med. Chem.* **2014**, *22*, 4049–4060. (d) Miller, M. J.; Cheng, J. Chemical syntheses and in vitro antibacterial activity of two desferrioxamine B-ciprofloxacin conjugates with potential esterase and phosphatase triggered drug release linkers. *Bioorg. Med. Chem.* **2012**, *20*, 3828–3836.

(27) For a desferridanoxamine-triclosan conjugate with a labile phenolic ester linker, see: Wencewicz, T. A.; Möllmann, U.; Long, T. E.; Miller, M. J. Is drug release necessary for antimicrobial activity of siderophore-drug conjugates? Syntheses and biological studies of the naturally occurring salmycin "Trojan Horse" antibiotics and synthetic desferridanoxamine-antibiotic conjugates. *BioMetals* **2009**, *22*, 633–648.

(28) Md-Saleh, S. R.; Chilvers, E. C.; Kerr, K. G.; Milner, S. J.; Snelling, A. M.; Weber, J. P.; Thomas, G. H.; Duhme-Klair, A.-K.; Routledge, A. Synthesis of citrate–ciprofloxacin conjugates. *Bioorg. Med. Chem. Lett.* **2009**, *19*, 1496–1498.

(29) Juárez-Hernández, R. E.; Miller, P. A.; Miller, M. J. Syntheses of Siderophore–Drug Conjugates Using a Convergent Thiol–Maleimide System. *ACS Med. Chem. Lett.* **2012**, *3*, 799–803.

(30) Wencewicz, T. A.; Miller, M. J. Biscatecholate–Monohydroxamate Mixed Ligand Siderophore–Carbacephalosporin Conjugates are Selective Sideromycin Antibiotics that Target *Acinetobacter baumannii*. *J. Med. Chem.* **2013**, *56*, 4044–4052.

(31) Wencewicz, T. A.; Long, T. E.; Möllmann, U.; Miller, M. J. . Trihydroxamate Siderophore–Fluoroquinolone Conjugates Are Selective Sideromycin Antibiotics that Target *Staphylococcus aureus*. *Bioconjugate Chem.* **2013**, *24*, 473–486.

(32) Milner, S. J.; Seve, A.; Snelling, A. M.; Thomas, G. H.; Kerr, K. G.; Routledge, A.; Duhme-Klair, A.-K. Staphyloferrin A as siderophore-component in fluoroquinolone-based Trojan horse antibiotics. *Org. Biomol. Chem.* **2013**, *11*, 3461–3468.

(33) Souto, A.; Montaos, M. A.; Balado, M.; Osorio, C. R.; Rodríguez, J.; Lemos, M. L.; Jiménez, C. Synthesis and antibacterial activity of conjugates between norfloxacin and analogues of the siderophore vanchrobactin. *Bioorg. Med. Chem.* **2013**, *21*, 295–302.

(34) Fardeau, S.; Dassonville-Klimpt, A.; Audic, N.; Sasaki, A.; Pillon, M.; Baudrin, E.; Mullié, C.; Sonnet, P. Probing linker design in citric acid–ciprofloxacin conjugates. *Bioorg. Med. Chem.* **2014**, *22*, 4049–4060.

(35) Zheng, T.; Nolan, E. M. Evaluation of (acyloxy)alkyl ester linkers for antibiotic release from siderophore-antibiotic conjugates. *Bioorg. Med. Chem. Lett.* **2015**, *25*, 4987–4991.

(36) Negash, K. H.; Norris, J. K. S.; Hodgkinson, J. T. Siderophore – Antibiotic conjugate design: New drugs for bad bugs? *Molecules* **2019**, *24*, 3314–3330.

(37) For an oxazolidinone-conjugated SAC with a non-cleavable linker, see: Paulen, A.; Hoegy, F.; Roche, B.; Schalk, I. J.; Mislin, G. L. A. Synthesis of conjugates between oxazolidinone antibiotics and a pyochelin analogue. *Bioorg. Med. Chem. Lett.* **2017**, *27*, 4867–4870.

(38) Neumann, W.; Sassone-Corsi, M.; Raffatellu, M.; Nolan, E. M. Esterase-catalyzed siderophore hydrolysis activates an enterobactin–ciprofloxacin conjugate and confers targeted antibacterial activity. *J. Am. Chem. Soc.* **2018***, 140,* 5193–5201.

(39) Neumann, W.; Nolan, E. M. *J. Biol. Inorg. Chem.* **2018***, 23,* 1025–1036.

(40) For a conjugate with a base-sensitive triazole-methylene carbamate linker, see: Paulen, A.; Gasser, V.; Hoegy, F.; Perraud, Q.; Pesset, B.; Schalk, I. J.; Mislin, G. L. A. Synthesis and antibiotic activity of oxazolidinone–catechol conjugates against Pseudomonas aeruginosa. *Org. Biomol. Chem.* **2015**, *13*, 11567–11579.

(41) Gupta, K.; Hooton, T. M.; Naber, K. G.; Wullt, B.; Colgan, R.; Miller, L. G.; Moran, G. J.; Nicolle, L. E.; Raz, R.; Schaeffer, A. J.; Soper, D. E. International Clinical Practice Guidelines for the Treatment of Acute Uncomplicated Cystitis and Pyelonephritis in Women: A 2010

Update by the Infectious Diseases Society of America and the European Society for Microbiology and Infectious Diseases. *Clin. Infect. Dis*. **2011**, *52*, e103–e120.

(42) Castro, W.; Navarro, M.; Biot, C. Medicinal potential of ciprofloxacin and its derivatives. *Future Med. Chem.* **2013**, *5*, 81–96.

(43) Choi, K. Y.; Swierczewska, M.; Lee, S.; Chen, X. Protease-activated drug development. *Theranostics* **2012**, *12*, 156–178.

(44) Baurain, R.; Masquelier, M.; Deprez-De Campeneere, D.; Trouet, A. Amino acid and dipeptide derivatives of daunorubicin. 2. Cellular pharmacology and antitumor activity on L1210 leukemic cells *in vitro* and *in vivo*. *J. Med. Chem.* **1980**, *23*, 1171–1174.

(45) For a recent review of protease-activated prodrugs, see: Poreba, M. Protease-activated prodrugs: strategies, challenges, and future directions. *FEBS J.* **2020**, https://doi.org/10.1111/febs.15227.

(46) Dubowchik, G.M.; Firestone, R. A.; Padilla, L.; Willner, D.; Hofstead, S. J.; Mosure, K.; Knipe, J. O.; Lasch, S. J.; Trail P. A. . Cathepsin B-labile dipeptide linkers for lysosomal release of doxorubicin from internalizing immunoconjugates: model studies of enzymatic drug release and antigen-specific in vitro anticancer activity. *Bioconjug. Chem.* **2002**, *13*, 855–869.

(47) Dubowchik, G. M.; Firestone, R. A. Cathepsin B-sensitive dipeptide prodrugs. 1. A model study of structural requirements for efficient release of doxorubicin. *Bioorg. Med. Chem. Lett.* **1998**, *8*, 3341–3346.

(48) Dubowchik, G.M.; Mosure, K.; Knipe, J. O.; Firestone, R. A. Cathepsin B-sensitive dipeptide prodrugs. 2. Models of anticancer drugs paclitaxel (Taxol), mitomycin C and doxorubicin. *Bioorg. Med. Chem. Lett.* **1998**, *8*, 3347–3352.

(49) Zhu, L.; Wang, T.; Perche, F.; Taigind, A.; Torchilin, V. P. Enhanced anticancer activity of nanopreparation containing an MMP2-sensitive PEG-drug conjugate and cell-penetrating moiety. *Proc. Natl. Acad. Sci. U.S.A*. **2013**, *110*, 17047–17052.

(50) an Duijnhoven, S. M.; Robillard, M. S.; Nicolay, K.; Grull, H. Tumor targeting of MMP-2/9 activatable cell-penetrating imaging probes is caused by tumor-independent activation. *J. Nucl. Med.*, **2011**, *52*, 279–286.

(51) Zhang, X.; Wang, X.; Zhong, W.; Ren, X.; Sha, X.; Fang, X. Matrix metalloproteinases-2/9-sensitive peptide-conjugated polymer micelles for site-specific release of drugs and enhancing tumor accumulation: preparation and *in vitro* and *in vivo* evaluation. *Int. J. Nanomed*. **2016**, *11*, 1643–1661.

(52) Kramer, L.; Turk, D.; Turk, B. The future of cysteine cathepsins in disease management. *Trends Pharmacol. Sci.* **2017**, *38*, 873–898.

(53) Liu, C.; Sun, C.; Huang, H.; Janda, K.; Edgington, T. Overexpression of legumain in tumors is significant for invasion/metastasis and a candidate enzymatic target for prodrug therapy. *Cancer Res*. **2003**, *63*, 2957–2964.

(54) Matsuo, K.; Kobayashi, I.; Tsukuba, T.; Kiyoshima, T.; Ishibashi, Y.; Miyoshi, A.; Yamamoto, K., Sakai, H. Immunohistochemical localization of cathepsins D and E in human gastric cancer: a possible correlation with local invasive and metastatic activities of carcinoma cells. *Hum. Pathol*. **1996**, *27*, 184–190.

(55) Toss, M. S.; Miligy, I. M.; Haj-Ahmad, R.; Gorringe, K. L.; AlKawaz, A.; Mittal, K.; Ellis, I. O.; Green, A. R.; Rakha, E. A. The prognostic significance of lysosomal protective protein (cathepsin A) in breast ductal carcinoma in situ. *Histopathology* **2019**, *74*, 1025–1035.

(56) Krinick, N. L.; Sun, Y.; Joyner, D.; Spikes, J. D.; Straight, R. C.; Kopecek, J. A polymeric drug delivery system for the simultaneous delivery of drugs activatable by enzymes and/or light. *J. Biomater. Sci. Polym. Ed.* **1994**, *5*, 303–324.

(57) Bajjuri, K. M.; Liu, Y.; Liu, C.; Sinha, S. C. The legumain protease-activated auristatin prodrugs suppress tumor growth and metastasis without toxicity. *ChemMedChem* **2011**, *6*, 54–59.

(58) Stern, L.; Perry, R.; Ofek, P.; Many, A.; Shabat, D.; Satchi-Fainaro, R. A novel antitumor prodrug platform designed to be cleaved by the endoprotease legumain. *Bioconjug. Chem.* **2009**, *20*, 500–510.

(59) Madu, C. O.; Lu, Y. *J.* Novel diagnostic biomarkers for prostate cancer. *Cancer*, **2010**, *1*, 150–177.

(60) Papsidero, L. D.; Wang, M. C.; Valenzuela, L. A.; Murphy, G. P.; Chu, T. M. A prostate antigen in sera of prostatic cancer patients. *Cancer Res.* **1980**, *40*, 2428–2432.

(61) Mahato, R.; Tai, W.; Cheng, K. Prodrugs for improving tumor targetability and efficiency. *Adv. Drug Deliv. Rev.* **2011**, *63*, 659–670.

(62) Chung, S. W.; Choi, J. U.; Cho, Y. S.; Kim, H. R.; Won, T. H.; Dimitrion, P.; Jeon, O-C.; Kim, S. W.; Kim, I-S.; Kim, S. Y.; Byun, Y. . Self-triggered apoptosis enzyme prodrug therapy (STAEPT): enhancing targeted therapies via recurrent bystander killing effect by exploiting caspase-cleavable linker. *Adv Sci (Weinh)* **2018**, *5*, 1800368.

(63) Law, C. L.; Cerveny, C. G.; Gordon, K. A.; Klussman, K.; Mixan, B. J.; Chace, D. F.; Meyer, D. L.; Doronina, S. O.; Siegall, C. B.; Francisco, J. A.; Senter, P. D.; Wahl, A. F. Efficient elimination of B-lineage lymphomas by anti-CD20-auristatin conjugates. *Clin. Cancer Res.* **2004**, *10*, 7842–7851.

(64) Diamantis, N.; Banerji, U. Antibody-drug conjugates–an emerging class of cancer treatment. *Br J Cancer* **2016**, *114*, 362–367.

(65) Weidle, U. H.; Tiefenthaler, G.; Georges, G. Proteases as activators for cytotoxic prodrugs in antitumor therapy. *Cancer Genomics Proteomics* **2014**, *11*, 67–79.

(66) Senter, P. D.; Sievers, E. L. The discovery and development of brentuximab vedotin for use in relapsed Hodgkin lymphoma and systemic anaplastic large cell lymphoma. *Nat. Biotechnol.* **2012**, *30*, 631–637.

(67) Deeks, E. D. Polatuzumab vedotin: first global approval. *Drugs* **2019**, *79*, 1467–1475.

(68) Beck, A.; Goetsch, L.; Dumontet, C.; Corvaia, N. Strategies and challenges for the next generation of antibody-drug conjugates . *Nat. Rev. Drug Discov.* **2017**, *16*, 315–337.

(69) Jeffrey, S. C.; Nguyen, M. T.; Andreyka, J. B.; Meyer, D. L.; Doronina, S. O.; Senter, P. D. Dipeptide-based highly potent doxorubicin antibody conjugates. *Bioorg. Med. Chem. Lett.* **2006**, *16*, 358–362.

(70) Lehar, S. M.; Pillow, T.; Xu, M.; Staben, L.; Kajihara, K. K.; Vandlen, R.; DePalatis, L.; Raab, H.; Hazenbos, W. L.; Morisaki, J. H.; Kim, J.; Park. S.; Darwish, M.; Lee, B. C.; Hernandez, H.; Loyet, K. M.; Lupardus, P.; Fong, R.; Yan, D.; Chalouni, C.; Luis, E.; Khalfin, Y.; Plise, E.; Cheong, J.; Lyssikatos, J. P.; Strandh, M.; Koefoed, K.; Andersen, P. S.; Flygare, J. A.; Wah Tan, M.; Brown, E. J.; Mariathanas, S. Novel antibody-antibiotic conjugate eliminates intracellular *S. aureus*. *Nature* **2015**, *527*, 323–328.

(71) Mariathasan, S.; Tan, M. W. Antibody-antibiotic conjugates: a novel therapeutic platform against bacterial infections. *Trends Mol. Med.* **2017**, *23*, 135–149.

(72) de Groot, F. M.; Broxterman, H. J.; Adams, H. P.; van Vliet, A.; Tesser, G. I.; Elderkamp, Y.W.; Schraa, A. J.; Kok, R. J.; Molema, G.; Pinedo, H. M.; Scheeren, H. W. Design, synthesis, and biological evaluation of a dual tumor-specific motive containing integrin-targeted plasmin-cleavable doxorubicin prodrug. *Mol. Cancer Ther*. **2002**, *1*, 901–911.

(73) Vhora, I.; Patil, S.; Bhatt, P.; Misra, A. Protein- and peptide-drug conjugates: an emerging drug delivery technology. *Adv. Protein Chem. Struct. Biol*. **2015**, *98*, 1–55.

(74) Zheng, G.; Chen, J.; Stefflova, K.; Jarvi, M.; Li, H.; Wilson, B. C. Photodynamic molecular beacon as an activatable photosensitizer based on protease-controlled singlet oxygen quenching and activation. *Proc. Natl. Acad. Sci. U.S.A.* **2007**, *104*, 8989–8994.

(75) Lo, P. C.; Chen, J.; Stefflova, K.; Warren, M. S.; Navab, R.; Bandarchi, B.; Mullins, S.; Tsao, M.; Cheng, J. D.; Zheng, G. Photodynamic molecular beacon triggered by fibroblast activation protein on cancer-associated fibroblasts for diagnosis and treatment of epithelial cancers. *J. Med. Chem.* **2009**, *52*, 358–368.

(76) Ivry, S. L.; Meyer, N. O.; Winter, M. B.; Bohn, M. F.; Knudsen, G. M.; O'Donoghue, A. J.; Craik, C. S. Global substrate specificity profiling of post-translational modifying enzymes. *Protein Sci.* **2018**, *27*, 584–594.

(77) Poreba, M.; Drag, M. Current strategies for probing substrate specificity of proteases. *Curr. Med. Chem.* **2010** *17*, 3968–3995.

(78) Janssen, S.; Jakobsen, C. M.; Rosen, D. M.; Ricklis, R. M.; Reineke, U.; Christensen, S. B.; Lilja, H.; Denmeade, S. R. Screening a combinatorial peptide library to develop a human glandular kallikrein 2-activated prodrug as targeted therapy for prostate cancer . *Mol. Cancer Ther.* **2004**, *3*, 1439–1450.

(79) Thornberry, N. A.; Rano, T. A.; Peterson, E. P.; Rasper, D. M.; Timkey, T.; Garcia-Calvo, M.; Houtzager, V. M.; Nordstrom, P. A.; Roy, S.; Vaillancourt, J. P.; Chapman, K. T.; Nicholson, D. W. A combinatorial approach defines specificities of members of the caspase family and granzyme B. Functional relationships established for key mediators of apoptosis. *J. Biol. Chem.* **1997**, *272*, 17907–17911.

(80) Choe, Y.; Leonetti, F.; Greenbaum, D. C.; Lecaille, F.; Bogyo, M.; Bromme, D.; Ellman, J. A.; Craik, C. S. Substrate profiling of cysteine proteases using a combinatorial peptide library identifies functionally unique specificities. *J. Biol. Chem.* **2006**, *281*, 12824–12832.

(81) Matthews, D. J.; Wells, J. A. Substrate of protease substrates by monovalent phage display. *Science* **1993**, *260*, 1113–1117.

(82) Newman, M. R.; Benoit, D. S. In Vivo Translation of Peptide-Targeted Drug Delivery Systems Discovered by Phage Display. *Bioconjugate Chem.* **2018**, *29*, 2161–2169.

(83) O'Donoghue, A. J.; Eroy-reveles, A. A.; Knudsen, G. M.; Ingram, J.; Zhou, M.; Statnekov, J. B.; Greninger, A. L.; Hostetter, D. R.; Qu, G.; Maltby, D. A.; Anderson, M. O.; DeRisi, J. L., McKerrow, J. H., Burlingame AL, Craik, C. S. Global identification of peptidase specificity by multiplex substrate profiling. *Nat Methods* **2012**, *9*, 1095–1100.

(84) Li, H.; O'Donoghue, A. J.; van der Linden, W. A.; Stanley, C. X.; Yoo, E.; Ian, T. F.; Leann, T.; Craik, C. S.; da Fonseca, P. C. A.; Bogyo, M. Structure- and function-based design of Plasmodium-selective proteasome inhibitors. *Nature* **2016**, *530*, 233–236.

(85) Lapek, J. D. Jr., Jiang, Z.; Wozniak, J. M.; Arutyunova, E.; Wang, S. C.; Lemieux, M. J.; Gonzalez, D. J.; O'Donoghue, A. J. Quantitative Multiplex Substrate Profiling of Peptidases by Mass Spectrometry. *Mol. Cell. Proteomics*, **2019**, *18*, 968–981.

(86) Vizovisek, M.; Vidmar, R.; Drag, M.; Fonovic, M.; Salvesen, G. S.; Turk B. Protease specificity: towards in vivo imaging applications and biomarker discovery. *Trends Biochem. Sci.* **2018**, *43*, 829–844.

(87) Chen, S.; Yim, J. J.; Bogyo, M. Synthetic and biological approaches to map substrate specificities of proteases. *Biol. Chem.*, **2019**, *401*, 165–182.

(88) Vizovisek, M,; Vidmar, R.; Fonovic, M.; Turk, B. Current trends and challenges in proteomic identification of protease substrates. *Biochimie* **2016**, *122*, 77–87.

(89) Sobotic, B.; Vizovisek, M.; Vidmar, R.; Van Damme, P.; Gocheva, V.; Joyce, J. A.; Gevaert, K.; Turk, V.; Turk, B.; Fonovic, M. Proteomic identification of cysteine cathepsin substrates shed from the surface of cancer cells. *Mol. Cell. Proteomics* **2015**, *14*, 2213–2228.

(90) Biniossek, M. L.; Niemer, M.; Maksimchuk, K.; Mayer, B.; Fuchs, J.; Huesgen, P. F.; McCafferty, D. G.; Turk, B.; Fritz, G.; Mayer, J.; Haecker, G.; Mach, L.; Schilling, O. Identification of protease specificity by combining proteome-derived peptide libraries and quantitative proteomics. *Mol. Cell. Proteomics* **2016**, *15*, 2515–2524.

(91) For studies investigating phage display to design peptide conjugates for targets such as whole cell or protein mixtures, see: (a) Laakkonen, P.; Akerman, M. E.; Biliran, H.; Yang, M.; Ferrer, F.; Karpanen, T.; Hoffman, R. M.; Ruoslahti, E. Antitumor activity of a homing peptide that targets tumor lymphatics and tumor cells. *Proc. Natl. Acad. Sci. U.S.A.* **2004**, *101*, 9381–9386. (b) Laakkonen, P.; Porkka, K.; Hoffman, J. A.; Ruoslahti, E. A tumor-homing peptide with a targeting specificity related to lymphatic vessels. *Nat. Med.* **2002**, *8*, 751–755. (c) Jin, W.; Qin, B.; Chen, Z.; Liu, H.; Barve, A.; Cheng, K. Discovery of PSMA-specific peptide ligands for targeted drug delivery. *Int. J. Pharm.* **2016**, *513*, 138–147. (d) Cieslewicz, M.; Tang, J.; Yu, J. L.; Cao, H.; Zavaljevski, M.; Motoyama, K.; Lieber, A.; Raines, E. W.; Pun, S. H. Targeted delivery of proapoptotic peptides to tumor-associated macrophages improves survival. *Proc. Natl. Acad. Sci. U.S.A.* **2013**, *110*, 15919–15924. (e) Liu, J.; Liu, J.; Chu, L.; Wang, Y.; Duan, Y.; Feng, L.; Yang, C.; Wang, L.; Kong, D.

Novel peptide-dendrimer conjugates as drug carriers for targeting nonsmall cell lung cancer. *Int. J. Nanomedicine* **2010**, *6*, 59–69. (f) Lempens, E. H.; Merkx, M.; Tirrell, M.; Meijer, E. W. Dendrimer display of tumor-homing peptides. *Bioconjug. Chem.* **2011**, *22*, 397–405.

(92) (a) Whitney, M.; Crisp, J. L.; Olson, E. S.; Aguilera, T. A.; Gross, L. A.; Ellies, L. G.; Tsien, R. Y. Parallel in vivo and in vitro selection using phage display identifies protease-dependent tumor-targeting peptides. *J. Biol. Chem.* **2010**, *285*, 22532–22541. (b) Cloutier, S. M.; Kündig, C.; Gygi, C. M.; Jichlinski, P.; Leisinger, H. J.; Deperthes, D. Profiling of proteolytic activities secreted by cancer cells using phage display substrate technology. *Tumor Biol.*, **2004**, *25*, 24–30.

(93) Kasperkiewicz, P.; Poreba, M.; Groborz, K.; Drag, M. Emerging challenges in the design of selective substrates, inhibitors and activity-based probes for indistinguishable proteases. *FEBS J.* **2017**, *284*, 1518–1539.

(94) Kisselev, A. F.; Goldberg, A. L. Proteasome inhibitors: from research tools to drug candidates. *Chem. Biol.* **2001**, *8*, 739–758.

(95) Caculitan, N. G.; Dela Cruz Chuh, J.; Ma, Y.; Zhang, D.; Kozak, K. R.; Liu, Y.; Pillow, T. H.; Sadowsky, J.; Cheung, T. K.; Phung, Q.; Haley, B.; Lee, B. C.; Akita, R. W.; Sliwkowski, M. X.; Polson, A. G. Cathepsin B is dispensable for cellular processing of cathepsin B-cleavable antibody-drug conjugates. *Cancer Res.* **2017**, *77*, 7027–7037.

(96) Akkari, L.; Gocheva, V.; Quick, M. L.; Kester, J. C.; Spencer, A. K.; Garfall, A. L.; Bowman, R. L.; Joyce, J. A. Combined deletion of cathepsin protease family members reveals compensatory mechanisms in cancer. *Genes Dev.*, **2016**, *30*, 220–232.

(97) Kay, B. K., Thai, S.; Volgina, V. V. High-throughput biotinylation of proteins. In: *High Throughput Protein Expression and Purification*; Doyle S.A., Eds.; Methods in Molecular Biology, vol *498*: Humana Press: Totowa, NJ, **2009**; pp. 185–196.

(98) Fairhead, M.; Howarth, M. Site-specific biotinylation of purified proteins using BirA. *Methods Mol. Biol.* **2015**, *1266*, 171–184.

(99) Neu, H. C.; Heppel, L. A. The release of enzymes from *Escherichia coli* by osmotic shock and during the formation of spheroplasts. *J. Chem. Biol.* **1965**, *240*, 3685–3692.

(100) See supporting information for complete experimental details.

(101) Lin, K-H.; Nalivaika, E. A.; Prachanronarong, K. L.; Yilmaz, N. K.; Schiffer, C. A. Dengue protease substrate recognition: binding of the prime side. *ACS Infect. Dis.* **2016**, *2*, 734–743.

(102) Zhong, Y-J.; Shao, L-H.; Li, Yan. Cathepsin B-cleavable doxorubicin prodrugs for targeted cancer therapy. *Int. J. Oncol.*, **2013**, *42*, 373–383.

(103) Harris, J. L.; Backes, B. J.; Leonetti, F.; Mahrus, S.; Ellman, J. A.; Craik, C. S. Rapid and general profiling of protease specificity by using combinatorial fluorogenic substrate libraries. *Proc. Natl. Acad. Sci. U. S. A.* **2000**, *97*, 7754–7759.

(104) Maly, D. J.; Leonetti, F.; Backes, B. J.; Dauber, D. S.; Harris, J. L.; Craik, C. S.; Ellman, J. A. Expedient solid-phase synthesis of fluorogenic protease substrates using the 7-amino-4-carbamoylmethylcoumarin (ACC) fluorophore. *J. Org. Chem.*, **2002**, *67*, 910–915.

(105) (a) Mensa, B.; Howell, G. L.; Scott, R.; DeGrado, W. F. Comparative Mechanistic Studies of Brilacidin, Daptomycin, and the Antimicrobial Peptide LL16. *Antimicrob. Agents Chemother*. **2014**, *58*, 5136–514. (b) Beriashvili, D.; Taylor, R.; Kralt, B.; Abu Mazen, N.; Taylor, S. D.; Palmer, M. Mechanistic Studies on the Effect of Membrane Lipid Acyl Chain Composition on Daptomycin Pore Formation. *Chem. Phys. Lipids* **2018**, *216*, 73–79. (c) Müller, A.; Wenzel, M.; Strahl, H.; Grein, F.; Saaki, T. N. V.; Kohl, B.; Siersma, T.; Bandow, J. E.; Sahl, H.-G.; Schneider, T.; Hamoen, L. W. Daptomycin Inhibits Cell Envelope Synthesis by Interfering With Fluid Membrane Microdomains. *Proc. Natl. Acad. Sci. U. S. A*. **2016**, *113*, E7077–E7086. (d) Hill, J.; Siedlecki, J.; Parr, I.; Morytko, M.; Yu, X.; Zhang, Y.; Silverman, J.; Controneo, N.; Laganas, V.; Li, T.; Lai, J. J.; Keith, D.; Shimer, G.; Finn, J. Synthesis and Biological Activity of N-Acylated Ornithine Analogues of Daptomycin. *Bioorg. Med. Chem. Lett*. **2003**, *13,* 4187–4191.

(106) Ghosh, M.; Miller, M. J. Design, synthesis, and biological evaluation of isocyanurate-based antifungal and macrolide antibiotic conjugates: iron transport-mediated drug delivery. *Bioorg. Med. Chem.* **1995**, *3*, 1519–1525.

(107) Daher, S. S.; Jin, X.; Patel, J.; Freundlich, J. S.; Buttaro, B.; Andrade, R. B. Synthesis and biological evaluation of solithromycin analogs against multidrug resistant pathogens. *Bioorg. Med. Chem. Lett.* **2019**, *29,* 1386–1389.

(108) Bellenger, J-P.; Arnaud-Neu, F.; Asfari, Z.; Myneni, S. C. B.; Stiefel, E. I.; Kraepiel, A. M. L. Complexation of oxoanions and cationic metals by the biscatecholate siderophore azotochelin. *J. Biol. Inorg. Chem.* **2007***,* *12*, 367–376.

(109) (a) Delorme, D.; Houghton, T.; Lafontaine, Y.; Tanaka, K.; Deitrick, E.; Kang, T.; Rafai Far, A. Phosphonated Oxazolidinones and Uses Thereof for the Prevention and Treatment of Bone and Joint Infections. Int. Patent Application PCT/IB2006/004233, December 6, 2006. (b) Miller, M. J.; McKee, J. A.; Minnick, A. A.; Dolence, E. K. The Design, Synthesis and Study of Siderophore-Antibiotic Conjugates. Siderophore Mediated Drug Transport. *Biol. Metals* **1991**, *4*, 62.

(110) Carmona, G.; Rodriguez, A.; Juarez, D.; Corzo, G.; Villegas, E. Improved protease stability of the antimicrobial peptide Pin2 substituted with D-amino acids. *Protein J.* **2013**, *32*, 456–466.

(111) Zheng, T.; Bullock, J. L.; Nolan, E. M. Siderophore-mediated cargo delivery to the cytoplasm of escherichia coli and pseudomonas aeruginosa: syntheses of monofunctionalized enterobactin scaffolds and evaluation of enterobactin−cargo conjugate uptake. *J. Am. Chem. Soc.* **2012**, *134*, 18388–18400.

(112) Sklar, J. G.; Wu, T.; Kahne, D.; Silhavy, T. J. Defining the roles of the periplasmic chaperones SurA, Skp, and DegP in *Escherichia coli. Genes Dev.* **2007**, *21*, 2473–2484.

(113) (a) Hagan, C. L.; Kim, S.; Kahne, D. Reconstitution of Outer Membrane Protein Assembly From Purified Components *Science* **2010**, *320*, 890–892. (b) Mahoney, T. F.; Ricci, D. P.; Silhavy, T. J. Classifying ß-barrel assembly substrates by manipulating essential Bam complex members. *J. Bacteriol.* **2016**, *198*, 1984–1992.

(114) Dubowchik, G. M.; Firestone, R. A. Cathepsin B-sensitive dipeptide prodrugs. 1. A model study of structural requirements for efficient release of doxorubicin. *Bioorg. Med. Chem. Lett.* **1998**, *1*, 3341–3346.

(115) Mikkelsen, H.; McMullan, R.; Filloux, A. The *Pseudomonas aeruginosa* reference strain PA14 displays increased virulence due to a mutation in ladS. *PLoS One*. **2011**, *6*, e29113.

(116) Knight, D. B.; Rudin, S. D.; Bonomo, R. A.; Rather, P. N. *Acinetobacter nosocomialis*: Defining the role of efflux pumps in resistance to antimicrobial therapy, surface motility, and biofilm formation. *Front. Microbiol.* **2018**, *9,* 1902.

(117) Chen, T. L.; Lee, Y. T.; Kuo, S. C.; Yang, S. P.; Fung, C. P.; Lee, S. D. Rapid identification of *Acinetobacter baumannii*, *Acinetobacter nosocomialis* and *Acinetobacter pittii* with a multiplex PCR assay. *J. Med. Microbiol.* **2014**, *63*, 1154–1159.

(118) Randall, C. P.; Mariner, K. R.; Chopra, I.; O'Neill, A. J. The target of daptomycin is absent from *Escherichia coli* and other gram-negative pathogens. *Antimicrob. Agents Chemother.* **2013**, *75*, 637–639.

(119) (a) Miller, C. G. Peptidases and Proteases of Escherichia Coli and Salmonella Typhimurium. *Annu Rev Microbiol.* **1975**, *29***,** 485–504. (b) Lazdunsk, A. M. Peptidases and proteases of *escherichia coli* and *salmonella typhimurium*. *FEMS Microbiol. Rev.* **1989**, *63*, 265–276.

(120) (a) Koehbach, J.; Craik, D. J. The vast structural diversity of antimicrobial peptides. *Trends Pharmacol. Sci*. **2019**, *40*, 517–528. (b) Lai, P. K., Tresnak, D. T., Hackel, B. J. Identification and elucidation of proline-rich antimicrobial peptides with enhanced potency and delivery. *Biotechnol. Bioeng.* **2019**, *116*, 2439–2450. (c) Li, W. F.; Ma, G. X.; Zhou, X. X. Apidaecin-type peptides: biodiversity, structure-function relationships and mode of action. *Peptides* **2006**, *27*, 2350–2359.

(121) PDB ID: 4WWW